AIChE WILEY InterScience® DISCOVER SOMETHING GREAT

Modeling and Inferential Control of the Batch Acetylation of Cellulose

Anshul Dubey, Matthew J. Realff, Jay H. Lee, and F. Joseph Schork
School of Chemical and Biomolecular Engineering, Georgia Institute of Technology, Atlanta, GA 30332

Alessandro Butté
Institute of Chemical and Bioengineering, Zürich, CH-8093 Switzerland

Bernat Ollé
School of Chemical Engineering, Massachusetts Institute of Technology, Cambridge, MA 02139

Lawton E. Kizer
Celanese Acetate LLC, Narrow, VA 24124

DOI 10.1002/aic.10816

The batch acetylation of cellulose involves two main stages, acetylation followed by hydrolysis. Mathematical models were constructed for these processes using reaction parameters obtained from earlier publications. The two models were then combined, along with a model predicting the cellulose feedstock moisture content. The overall temperature profiles as well as the final degree of acetylation and polymerization were shown to match the data obtained from a commercial process. From the results of the model and the observations made in a typical process, it has been established that this process is highly sensitive to disturbances in the input streams that can result in unacceptable final properties of the batch. Because the exact disturbance occurring in a batch cannot be identified and measured, inferential control is used to formulate an intrabatch control strategy. Support vector regression is used to make predictions on the final properties of the batch. These predictions, along with the model of the hydrolysis stage, are used to estimate the inputs that, when applied during hydrolysis, can counter the disturbances caused during the acetylation stage. Simulations show that this hydrolysis control strategy can improve the average batch properties of cellulose acetate required for subsequent processing. © 2006 American Institute of Chemical Engineers *AIChE J,* 52: 2149–2160, 2006

Keywords: modeling, cellulose acetate, acetylation, support vector machines, model-based control, degradation of cellulose, hydrolysis of cellulose acetate

Introduction

Cellulose is a high molecular weight polymer composed of glucose units linked by β-1,4 linkages. Each glucose unit contains three free hydroxyl groups that are substituted by the acetyl groups during acetylation of cellulose to form cellulose acetate (Figure 1). Two of the hydroxyl groups (bottom of Figure 1) are secondary, whereas one is called the primary group. The acetylation is brought about by acetic anhydride and conforms to the following stoichiometry:

$$\text{Cell} - (\text{OH})_3 + 3\text{Ac}_2\text{O} \Leftrightarrow \text{Cell} - (\text{OAc})_3 + 3\text{AcOH} \quad (1)$$

Correspondence concerning this article should be addressed to J. H. Lee at jlee@chbe.gatech.edu.

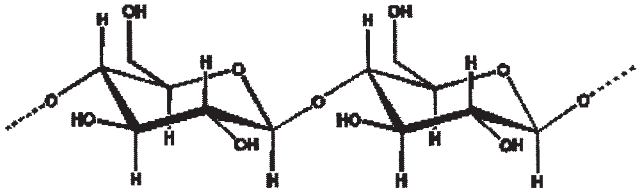

Figure 1. Cellulose units showing the hydroxyl groups.

The overall process of acetylation consists of two steps: acetylation followed by hydrolysis of the triester. Because cellulose exists in the solid phase and acetic anhydride is liquid, it creates a multiphase reaction system. Sulfuric acid is added to the reaction mixture to catalyze the acetylation. The average number of acetate groups present per molecule of cellulose can be called the *degree of acetylation* (DA), which can have a maximum value of 3 when all the hydroxyl groups have been substituted. Apart from acetylation, cellulose also undergoes random chain scission in the presence of sulfuric acid, causing a reduction of its *degree of polymerization* (DP), which is the average number of monomeric units in the polymer chains. After acetylation, cellulose is subjected to hydrolysis, which removes combined sulfate groups as well as some of the acetyl groups. Also, the DP is further reduced.

The DA and the DP of cellulose acetate, obtained at the end of hydrolysis, must meet the specifications required for subsequent processing. However, the acetylation process is highly sensitive to the disturbances in the input stream. For a batch process, such disturbances, which lead to changes in the final properties, will increase product variability or result in the whole batch being discarded. This creates a need for a comprehensive mathematical model that incorporates all that is known about the process. Such a model can be used by an effective control strategy that can restrain the final batch properties within the prescribed limits.

The reactions involved in this process, as well as the rate expressions and their enthalpy, have been individually investigated in both the open and the proprietary literature. A mathematical model was built, using mass and energy balances, for both the acetylation and the hydrolysis process. A model to predict the amount of moisture taken up by cellulose while being conveyed to the reactor vessel is also incorporated. The temperature profile and the final parameters of cellulose acetate, as predicted by the model, give an indication of its accuracy when compared with the observations from a commercial process. This creates a unified model of the whole process, which can predict the final properties of cellulose acetate, such as the degrees of acetylation and polymerization, from the inputs of each step.

The unified model described here appears to be the first of its nature for batch cellulose acetylation, which combines the relevant studies made on the reactions of the process. However, besides the reactions there are several other features of the process that are not fully explained, such as the mechanism of the dissolution of the cellulose fibers. The process is also known to be extremely sensitive to the temperature profile and requires a precise energy balance in the model, which implies that, along with the enthalpy of the reactions, other factors such as heat transfer and the melting of any ice crystals in the initial reaction mixture need to be modeled accurately.

A feasible intrabatch control strategy that can be developed using the process model is inferential control,[1,2] which uses a machine learning algorithm to predict the outcome of the batch or the primary variables from the observed or the secondary variables. This prediction can be used along with a nonlinear control of the system.[3] Note that the control strategy is independent of the machine learning algorithm used. Different machine learning strategies, predominantly Artificial Neural Networks, have been used for the prediction of primary variables.[3,4]

The recently developed Support Vector Machines (SVMs)[5,6] learning algorithm is based on Statistical Learning Theory (SLT). Data points are mapped from the input space to the higher-dimensional feature space, using a *kernel*, where it can be fit by a linear function. The linear function is obtained by minimizing the upper bound on the generalization error. The number of parameters involved in this function is fixed to be equal to the size of the data set used for training, which thus avoids overfitting the data by using more parameters than required. SVMs have been widely applied in the field of pattern recognition such as face recognition.[7,8] They have also been applied as the estimating algorithm for process control applications.[9,10]

In this article, we have chosen to use Support Vector Regression (SVR), which was used in predicting the DA and DP of cellulose acetate at the end of process from the observed variables of acetylation. The process model was used to create the training data set. A Multilayer Perceptron Neural Network regression with a single hidden layer was also used to make the same predictions. On comparing the two algorithms, over the same test data set, SVR was found to give a better overall performance. An optimal control strategy was designed, using the model of the hydrolysis process alone, which uses this prediction to determine the quantity of the input streams to be added during hydrolysis for the final batch properties to comply with the specifications. This strategy was simulated using the process model and the results show a significant improvement in the batch quality when compared with the baseline conditions.

Process Description

Acetylation

The first step in the process is acetylation of cellulose. Shredded cellulose is transferred to the reactor vessel using air conveying. Because the initial moisture content of the pulp is affected by the contact with air, a mass transfer model was also developed to predict the inlet moisture content of pulp after it has been in contact with air. A stream in a partially frozen state, consisting of sulfuric acid, acetic anhydride, and acetic acid, is added. When in contact with moisture in the pulp, acetic anhydride undergoes rapid hydrolysis that releases significant amounts of heat. Sulfuric acid helps to dissolve the solid pulp by substituting one of its hydroxyl groups by the sulfate group. The remaining acetic anhydride then substitutes the remaining hydroxyl groups of the dissolved chains of cellulose by the acetyl group (Figure 2). It also replaces the sulfate groups to a certain extent. The presence of sulfuric acid also reduces the degree of polymerization or the average chain length of cellulose by causing scission at random points in the chain. Because the acetylation reaction is exothermic in nature, the tempera-

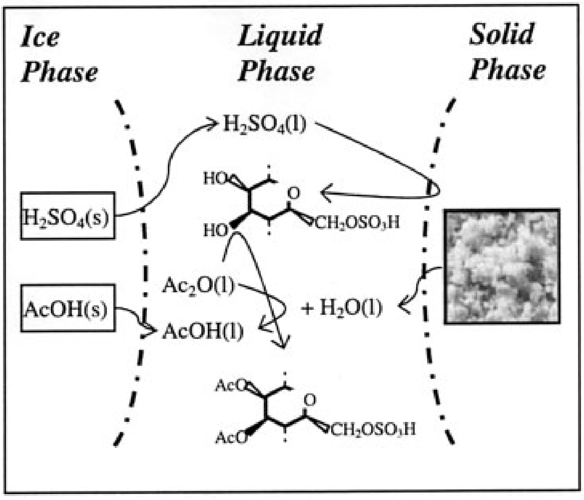

Figure 2. Acetylation process scheme showing the different chemical species and the physical states.

ture of the batch continues to increase and reaches a peak, referred to as the *peak temperature* from here on, when all the hydroxyl groups have been exhausted. The time when the peak temperature occurs is called the *peak time*. After a specific interval of additional reaction time, a neutralizer solution is added to quench the acetylation reaction. Because of the rapid hydrolysis of the leftover acetic anhydride, the temperature undergoes a sharp increase. A coolant is circulated in the jacket to help absorb the heat generated during the reactions.

Hydrolysis

After acetylation, the batch is transferred to another vessel for hydrolysis. Steam is used to further increase the temperature, up to a target final temperature. A feedback control loop operates the steam valve to ensure that the temperature reaches that target in the preset time and is maintained there. Separate neutralizer solutions are added at various intervals. The main purpose of hydrolysis is to remove the sulfate groups and reduce the number of acetyl groups attached to cellulose by replacing them with the hydroxyl groups (commercial cellulose acetate is <100% acetylated). The sulfate groups that are removed from cellulose acetate are neutralized by the neutralizer. The degree of polymerization is also reduced because of the high temperature.

Reaction Chemistry

Basic reactions

During acetylation and hydrolysis of cellulose, a number of reactions occur at a significant rate and are included in the model. The rate expressions and kinetic parameters for these reactions were obtained from the sponsors as well as external literature, although for proprietary reasons they are not included herein. The chemical equations for these reactions are represented by the following:

- The sulfation of solid cellulose:

$$\mathrm{Cell}-(\mathrm{OH})_3(s)+\mathrm{H_2SO_4}\rightarrow \mathrm{Cell}-(\mathrm{OH})_2-\mathrm{HSO_4}+\mathrm{H_2O} \tag{2}$$

This reaction occurs almost exclusively at the primary hydroxyl group of cellulose.

- Acetylation of cellulose acetate:

$$\mathrm{Cell}-(\mathrm{OH})_x-(\mathrm{HSO_4})_y-(\mathrm{OAc})_z+\mathrm{Ac_2O}\rightarrow \mathrm{Cell}-(\mathrm{OH})_{x-1}-(\mathrm{HSO_4})_y-(\mathrm{OAc})_{z+1}+\mathrm{AcOH} \tag{3}$$

This reaction is the same for different values of x, y, and z, which represent the number of the particular group.

- The hydrolysis of acetic anhydride:

$$\mathrm{Ac_2O}+\mathrm{H_2O}\rightarrow 2\mathrm{AcOH} \tag{4}$$

- The displacement of sulfate with the acetyl group:

$$\mathrm{Cell}-(\mathrm{OH})_x-(\mathrm{HSO_4})_y-(\mathrm{OAc})_z+\mathrm{Ac_2O}\rightarrow \mathrm{Cell}-(\mathrm{OH})_x-(\mathrm{HSO_4})_{y-1}-(\mathrm{OAc})_{z+1}+\mathrm{Ac}-\mathrm{HSO_4} \tag{5}$$

- The hydrolysis of the sulfate group:

$$\mathrm{Cell}-(\mathrm{OH})_x-(\mathrm{HSO_4})_y-(\mathrm{OAc})_z+\mathrm{H_2O}\rightarrow \mathrm{Cell}-(\mathrm{OH})_{x+1}-(\mathrm{HSO_4})_{y-1}-(\mathrm{OAc})_z+\mathrm{H_2SO_4} \tag{6}$$

- The hydrolysis of the acetyl group:

$$\mathrm{Cell}-(\mathrm{OH})_x-(\mathrm{HSO_4})_y-(\mathrm{OAc})_z+\mathrm{H_2O}\rightarrow \mathrm{Cell}-(\mathrm{OH})_{x+1}-(\mathrm{HSO_4})_y-(\mathrm{OAc})_{z-1}+\mathrm{AcOH} \tag{7}$$

- Sulfuric acid neutralization:

$$\mathrm{Neutralizer}+\mathrm{H_2SO_4}\rightarrow \mathrm{Sulfate\ salt} \tag{8}$$

Literature

It has been reported that sulfuric acid combines rapidly and quantitatively with cellulose when acetic anhydride is added; however, the acetylation of cellulose is comparatively slow.[11] The acetylation reaction is also shown to be slow, compared to sulfation, when cellulose is swollen as a result of the presence of acetic acid.[12,13] The mechanism of this reaction involves dissolution of layers of cellulose fiber after its sulfation so that new surface is exposed for further reaction.[14] The reaction is shown to be faster than acetylation at low temperatures.[12] The sulfation of the primary hydroxyl group is preferred over the secondary[11] and the reaction is reversible.[13] The kinetic expression reported in the proprietary literature is consistent with these observations.

The acetylation of cellulose is known to be catalyzed by sulfuric acid. The rate is higher for the primary group than for the secondary groups.[15] The hydrolysis of sulfate and acetyl groups also occurs at a significant rate. It is known that the hydrolysis of the sulfate groups is faster than that of the acetyl groups, whereas hydrolysis of the primary groups is more rapid than that of the secondary groups.[16] There is also evidence of a reaction that displaces the sulfate groups with the acetyl groups.[12] Acetic anhydride, and not acetic acid, is responsible for this reaction that can be assumed to follow a simple second-order mechanism and is much faster for the secondary groups.[11]

Cellulose chain scission is one of the most important side reactions during acetylation because it accounts for the critical loss in the degree of polymerization (DP) of cellulose. Very few data are available to firmly establish the rate expression for this reaction, but it is catalyzed internally by the sulfate groups attached to cellulose. An empirical rate expression, which includes the effect of sulfuric acid as a catalyst for this reaction, was used. This proprietary expression has been proven to make accurate predictions on the final degree of polymerization of cellulose.

Model Description and Assumptions

Moisture calculation during transport

The air conveyor used for transporting the pulp to the reactor vessel results in mass transfer, which affects the moisture content of the pulp. The extent of moisture change varies with the environmental conditions. Because the acetylation process is highly sensitive to the initial moisture content, accurately modeling the mass transfer is very critical.

The pulp in the conveyor was assumed to be in the form of a fluff consisting of aggregated particles that can be approximated to be spherical in shape. Using the known values of the flow rate of air in the conveyor as well as the duct dimensions, an order of magnitude study showed that external mass transfer is not limiting in this case. For spherical particles, the internal diffusion mass transfer equation can be written as

$$\frac{\partial C}{\partial t} = D_{eff}\left(\frac{\partial^2 C}{\partial r^2} + \frac{2}{r}\frac{\partial C}{\partial r}\right) \tag{9}$$

where C is the concentration of water in the pulp. Applying the boundary conditions, $C(r = a) = C_0$, constant concentration on the surface, and $\partial C/\partial r\,|_{r=0} = 0$, the analytical solution of this equation can be written as

$$\frac{C - C_i}{C_0 - C_i} = 1 + \frac{2a}{\pi r}\sum_{n=1}^{\infty}\frac{(-1)^n}{n}\sin\left(\frac{n\pi r}{a}\right)\exp\left(\frac{D_{eff}n^2\pi^2 t}{a^2}\right) \tag{10}$$

where C_0 is the concentration of water on the surface of the particle, which is assumed to be in equilibrium with the air in contact; C_i is the initial concentration assumed to be uniform inside the particle; and a is the diameter of the particle.

The data available for calculating the moisture content are the relative humidity and temperature of air at the inlet of the conveyor as well as the air temperature at the outlet. The inlet moisture content of pulp is assumed to be known. From Eq. 10 the final moisture content of the pulp, after accounting for the internal mass transfer limitation, can be calculated.

Acetylation

The model for acetylation was developed as a first-principle model using the mass and energy balances in the reactor. The mass balance equation for all the chemical species in the liquid phase of the reactor can be written generically as

$$\frac{dm_i}{dt} = \sum_j F_{i,j} + \sum_k \nu_{i,k}R_k \tag{11}$$

where m_i represents the moles of the ith species and $F_{i,j}$ represents the molar flow rates of that species in the jth stream. The different reactions are denoted by k and R_k represents the molar reaction rate with $\nu_{i,k}$ the stoichiometric coefficient of the species i. Note that, although not shown as a separate equation, the volume of the liquid phase (which is included in the reaction rate) is also a variable that changes as a result of the addition of different streams as well as transfer of mass from the solid (cellulose and ice crystals) to the liquid phase.

The change in enthalpy of the batch can be represented as

$$\frac{dH}{dt} = \sum_i\sum_j F_{i,j}c_{p,i}(T_j - T_{ref}) + \sum_l \dot{Q}_l \tag{12}$$

$$\Rightarrow \left[\sum_i c_{p,i}(T - T_{ref})\frac{dm_i}{dt} + \sum_i c_{p,i}m_i\frac{dT}{dt}\right] = \sum_i\sum_j F_{i,j}c_{p,i}(T_j - T_{ref}) + \sum_l \dot{Q}_l \tag{13}$$

where $c_{p,i}$ represents the molar specific heat capacity of the species i and T_{ref} and T_j denote a reference temperature and the temperature of the jth stream, respectively, and T is the batch temperature. $\dot{Q}_l$ represents all the other sources of heat including heat transfer from the jacket. Substituting the rates of the reactions R_k for dm_i/dt in Eq. 13, we obtain

$$\left(\sum_i c_{p,i}m_i\right)\frac{dT}{dt} = \sum_i\sum_j F_{i,j}c_{p,i}(T_j - T) + \sum_k R_k\Delta H_{r,k}(T) + \sum_l \dot{Q}_i \tag{14}$$

where $\Delta H_{r,k}(T)$ represents the enthalpy of the kth reaction at a temperature T. The term $\Sigma_i\, c_{p,i}m_i$ stands for the total heat capacity of the system. $\dot{Q}_l$ represents all the other heat sources/sinks and includes the heat spent in the melting of the initial ice phase as well as the heat transfer to the brine in the external jacket.

The model was written in FORTRAN using the Compaq Visual Fortran environment. The assumptions and methodology of modeling some peculiar aspects of acetylation are discussed in the following sections.

Initial Entry of Pulp. Before the pulp, a frozen mixture of acetic anhydride, sulfuric acid, and acetic anhydride is introduced into the reactor. This addition is assumed to be instantaneous. The pulp feed is assumed to occur at two stages: In the first stage pulp is added at a constant rate and in the second, the addition rate is slower. The pulp specifications such as diameter of fiber, density, and initial degree of polymerization must be given as input. With the entry of pulp in the reactor, the following events are initiated:

- The water in the pulp leads to hydrolysis of acetic anhydride and the energy liberated from this reaction leads to melting of the sulfuric acid and acetic acid crystals.
- The sulfuric acid starts to react with the hydroxyl groups of cellulose, mainly the primary group, leading to dissolution of the cellulose. This reaction takes place on the surface of the cellulose fiber and proceeds radially into the fiber. As a result, during the addition of cellulose, there is a radial distribution among the fibers in the reactor. To account for this distribution, the addition of cellulose was discretized so that fiber groups could be tracked separately.
- It is assumed that the dissolution of cellulose requires only a fraction of cellulose units to be sulfated. This assumption and the exact fraction were based on proprietary observation of a commercial process.
- Once in solution, the cellulose units are available for all the other reactions including acetylation.

Melting of Acetic Acid Crystals. Some of the acetic acid in the initial charge is known to be in the form of ice crystals at the inlet temperature. The melting of these crystals has been modeled using a mass transfer rate

$$R_{melt} = kS\Delta C = \frac{D}{r} 4\pi r^2 [C^{Eq}_{AAc}(T) - C^{(w)}_{AAc}] \qquad (15)$$

where $C^{Eq}_{AAc}(T)$ represents the equilibrium concentration of acetic acid (AAc), at the solid–liquid interface, at temperature T. It is obtained from the eutectic phase diagram, which gives the weight fraction of acetic acid in equilibrium as a function of temperature.

$$w^{Eq}_{AAc} = f(T) \qquad (16)$$

This equation is used to iteratively solve for the batch temperature. The latent heat for acetic acid and the initial mean radius of the ice crystals are given as input to the model. The heat transfer between the solid and the liquid phases is assumed to be fast and nonlimiting and heat required for melting is instantaneously obtained from the hydrolysis of acetic anhydride.

Heat Balance. The major heat source for the batch is the heat evolved from the reactions, primarily acetic anhydride hydrolysis and acetylation. The coolant circulating in the jacket serves as a heat sink and the overall heat transfer coefficient and surface area of contact depend on the geometry of the specific reactor. The coolant flow was assumed to be well mixed having a uniform temperature.

The heat taken up by the reactor walls is also significant and is taken into account. The heat transfer rate is assumed to be fast. This imparts a high heat capacity to the overall batch on the left-hand side in Eq. 14. It also includes the heat capacities of the initial solid phase of the reaction, which consists of the cellulose pulp and the ice crystals, which are also assumed to be at the same temperature as that of the batch. The heat generated by stirring (shaft work) is also significant given the viscous nature of the batch and is included in $\dot{Q}_l$ in Eq. 14. This value is approximated to be the difference in the power required by the stirring shaft for a full and an empty vessel.

Initially, before anything is added to the reactor, the vessel is assumed to be at a high temperature arising from the end of the previous batch. When the partially frozen stream is added, heat transfer takes place with the reactor walls and an equilibrium temperature is assumed to be achieved before the addition of pulp. This temperature is iteratively calculated by taking into account the melting of the ice crystals.

Hydrolysis

After acetylation, the batch is transferred to another vessel for hydrolysis. During hydrolysis, almost all of the sulfur groups and some of the acetyl groups in cellulose are replaced by the hydroxide group. The temperature is increased to further facilitate the process. A proprietary model for hydrolysis was provided and we created a second-generation version of that model with a few additions. The newer version of the model was written in FORTRAN.

The mass balance for the hydrolysis of cellulose is similar to Eq. 11 for all the species except water:

$$\frac{dm_w}{dt} = \sum_i F_{w,i} + \sum_k \nu_{w,k} R_k + \xi \frac{dT}{dt} \qquad (17)$$

where ξ, the steam required per unit increase of the batch temperature, is assumed to be constant. The heat balance is also similar to Eq. 14 with $\dot{Q}_l$ representing the heat added by the steam. The major reactions include hydrolysis of the acetyl and sulfate groups and the formation of sulfate salt.

Combined model of the process

The models for the acetylation and the hydrolysis of cellulose were combined to construct a model for the whole process. The calculation of the moisture content at the inlet before acetylation was also linked to the whole model. The batch parameters from after acetylation were transferred as input to the hydrolysis step and common process parameters were used. This combination allows the overall batch profiles to be observed and examined. The changes made during acetylation are reflected in the final product at the end of hydrolysis. An interface for the model was created using Visual Basic.

Model-Based Control

The acetylation step of cellulose is prone to many disturbances that affect the final product quality. Variations are frequently observed in the cellulose addition and also its initial moisture content. Changes like these in the input streams of acetylation are reflected in properties of the cellulose acetate obtained at the end of hydrolysis. However, by being divided into two subprocesses—acetylation and hydrolysis—this process provides an opportunity for intrabatch control.

During hydrolysis, a number of input streams are added, which include the neutralizer solutions and water. It has been observed from the model that disturbances caused during acetylation can be rectified in part by appropriate changes during hydrolysis. Hydrolysis is also less sensitive to disturbances in its inputs compared to acetylation. Based on these observations, a model-based control strategy can be applied to the hydrolysis process.

To be able to apply this intrabatch strategy, the variables to be controlled—the DA and DP for the end product—should be known before the batch is subjected to hydrolysis. The main observable parameter during acetylation is the batch temperature. It is known that the disturbances occurring during acetylation are reflected in the peak temperature, peak time, and the second temperature rise. These parameters have been used in industry to create batch-to-batch rules of thumb to control the process. The observations from the model confirm this behavior and also show a definite and unique correlation between these parameters and the final properties of the product obtained after hydrolysis. This suggests that a nonlinear regression can be applied to use the observations during acetylation and predict the DA and DP at the end of hydrolysis. Note that the process model does not provide the means to make this prediction without knowing the exact disturbances caused in the input streams during acetylation.

SVM regression

SVM regression is a highly effective nonlinear regression algorithm that is based on statistical learning theory.[6] Instead of fitting a nonlinear function in the input space, the data are transformed into a typically higher-dimensional *feature space* where the correlation between the data is linear. A linear regression is used to find an optimum hyperplane that fits the data in that space.

The input data is in the form of a vector $\mathbf{x}$ with an output y. The corresponding feature vector, for a transformation $\boldsymbol{\phi}$ to the feature space, is denoted by $\boldsymbol{\phi}(\mathbf{x})$. A kernel function is defined as the inner product of feature vectors:

$$K(\mathbf{x}_1, \mathbf{x}_2) = \boldsymbol{\phi}(\mathbf{x}_1) \cdot \boldsymbol{\phi}(\mathbf{x}_2) \tag{18}$$

From the duality theorem, the optimal hyperplane or the regression function that calculates the output y for a vector $\mathbf{x}$ is given by[5]

$$y = f(\mathbf{x}) = \sum_{i=1}^{\ell} \alpha_i^* K(\mathbf{x}_i, \mathbf{x}) + b^* \tag{19}$$

where $[(\mathbf{x}_1, y_1), \ldots, (\mathbf{x}_\ell, y_\ell)] = S$ is the training data set. The parameters $\boldsymbol{\alpha}^* = (\alpha_i^*, \ldots, \alpha_\ell^*)$, also called the Lagrangian variables, are the optimal solution of the following problem:

$$\text{Maximize } W(\boldsymbol{\alpha}) = \sum_{i=1}^{\ell} y_i \alpha_i - \varepsilon \sum_{i=1}^{\ell} |\alpha_i| - \frac{1}{2} \sum_{i=1}^{\ell} \sum_{j=1}^{\ell} \alpha_i \alpha_j K(\mathbf{x}_i, \mathbf{x}_j)$$

$$\text{subject to } \sum_{i=1}^{\ell} \alpha_i = 0 \qquad -C \le \alpha_i \le C \qquad i = 1, \ldots, \ell \tag{20}$$

This formulation corresponds to the linear ε-insensitive loss function (Figure 3). The value of ε is fixed depending on the problem. The bias, b^* in Eq. 19, is chosen so that $f(\mathbf{x}_i) - y_i = -\varepsilon$ for any i with $0 \le \alpha_i^* \le C$.

Note that to solve this problem and obtain $\boldsymbol{\alpha}^*$, only the kernel function for the feature space is required and not the feature vectors. This allows one to circumvent explicitly defining the feature space and, instead, define only a kernel function as the inner product of the feature space. For a function to qualify as a kernel, it should satisfy the properties of an inner product in any space, such as symmetry and the Cauchy–Schwarz inequality $[K(\mathbf{x}, \mathbf{z})^2 \le K(\mathbf{x}, \mathbf{x})K(\mathbf{z}, \mathbf{z})]$. According to Mercer's theorem, the kernel matrix, $\mathbf{K} = [K(\mathbf{x}_i, \mathbf{x}_j)]_{i,j=1}^{\ell}$, should also be positive semidefinite (have nonnegative eigenvalues).[5] Different forms of functions, which satisfy these properties, have been used for various problems. The polynomial kernel, $K(\mathbf{x}, \mathbf{z}) = (1 + \mathbf{x} \cdot \mathbf{z})^m$, where the order m can be varied, and the radial basis kernel, $K(\mathbf{x}, \mathbf{z}) = \exp(-\|\mathbf{x} - \mathbf{z}\|^2/\sigma^2)$, with the parameter σ defined as the width of the function, are frequently applied.

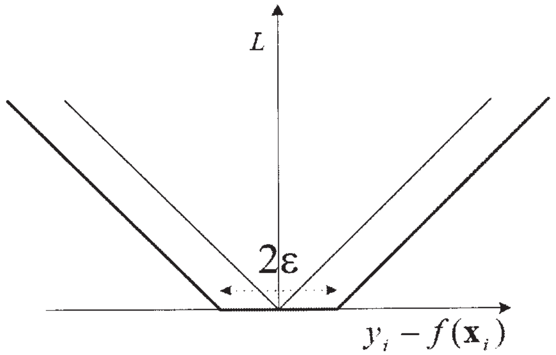

Figure 3. The ε-loss function plotted against the difference between the actual value and the prediction.

Hydrolysis-based control

The objective of the control algorithm is to minimize the deviation in the final properties of cellulose acetate: the degree of acetylation (DA) and the degree of polymerization (DP). Using SVM regression, these variables can be predicted from the observed parameters in acetylation. The parameters that can be manipulated are the amounts of input streams (neutralizer solutions and water) that should be added during hydrolysis. The following optimization loop can be used to evaluate the optimal amounts of the input streams:

$$\min \beta[DA_{target} - DA(x)]^2 + [DP_{target} - DP(x)]^2 \qquad \text{subject to } lb \le x \le ub \tag{21}$$

where x = [Amount of streams added]; β is a scaling factor; and lb and ub are, respectively, the lower and upper bounds applicable to the quantity of the input streams. The disturbance in the manipulated variables is assumed to be negligible. $DA(x)$ and $DP(x)$ can be obtained from the hydrolysis model for the given value of input streams x. However, to be able to use the hydrolysis model, the exact inputs during acetylation are also required because the properties of the batch before hydrolysis should be known. Because the disturbances during acetylation are generally unknown and the properties of the batch after acetylation are not measured online, this approach is infeasible. To overcome this difficulty a linear feedback assumption can be used:

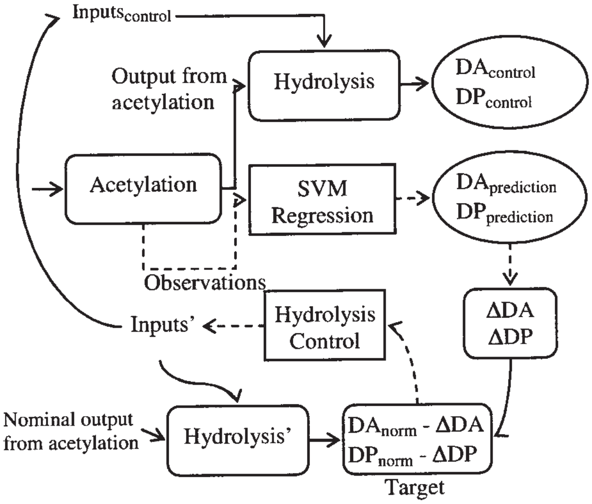

Figure 4. Hydrolysis-based control with a linearized assumption.

$$\min \alpha\{DA_{target} - [DA(a) - DA_{target}] - DA^{n}(x)\}^{2} + \{DP_{target} - [DP(a) - DP_{target}] - DP^{n}(x)\}^{2} \quad \text{subject to } lb \leq x \leq ub \qquad (22)$$

where $DA(a)$ and $DP(a)$ are the final properties of the batch when the nominal values of the input streams of hydrolysis, a, are used. These values can be predicted from the observations during acetylation using a nonlinear regression such as SVM regression. $DA^{n}(x)$ and $DP^{n}(x)$ are the degree of acetylation and the degree of polymerization obtained from the hydrolysis model using the input stream x and assuming that inputs for the acetylation are nominal without any disturbances. This strategy is explained as a block diagram in Figure 4. The observations from acetylation are used by SVM regression to predict the DA and DP of the output stream after hydrolysis. By comparing these values to the nominal DA and DP, we can obtain the offset, ΔDA and ΔDP. The model for hydrolysis is used in parallel with the nominal inputs (the stream obtained after acetylation without any disturbances). The hydrolysis control loop is used to evaluate the quantities of the inputs required to counter the offset predicted by regression but starting from the nominal values of DA_{norm} and DP_{norm}. For example, if the regression predicts the degree of polymerization to be 10% above normal, the optimization loop finds the optimal inputs x that offset the degree of polymerization, as predicted by the model, to 10% *below* normal. If the hydrolysis model can be assumed to be linear, then using these quantities of the inputs in the actual hydrolysis process will bring the outputs as close to the nominal values as is possible under the applied constraints and give results comparable to the optimization loop in Eq. 21. In reality, however, because of the nonlinear nature of the model, the results will be poorer than those obtained using the more direct but infeasible approach shown in Eq. 21.

Results and Discussion

Modeling

Pulp Moisture Calculation. The final moisture content of the pulp was predicted at the outlet for two different air conveyor ducts of different lengths. The model results are compared with the moisture contents measured in the plant in Table 1. The predictions match well with the measurements made in the plant. It should be noted, however, that the model is based entirely on mass balance and internal diffusion limitations and is sensitive to the measurement of the relative humidity of air and also its outlet temperature. Also, the predictions of this model have been tested for only a limited range of conditions.

Table 1. Moisture Predictions for Two Different Air Conveyors

Unit	Length of Duct (ft)	Initial Moisture (%)	Observed Moisture (%)	Predicted Moisture (%)
1	L_1	7.53	7.33	7.33
2	L_2	7.78	7.42	7.45

Acetylation. The temperature profile obtained from the model is plotted along with profiles from two commercial batches in Figure 5. The axes have been filtered with a nonlinear technique. This is done to preserve the confidentiality of proprietary data. However, the main purpose of this figure is to show the accuracy of the model in matching the observed profile. The final properties of cellulose acetate are highly sensitive to the peak temperature and the peak time observed during acetylation. As can be seen from Figure 5, the peak temperature and the peak time are very well predicted by the model. The initial temperature of the batch, calculated as the equilibrium between the hot walls of the batch and frozen mixture, coincides with the observation. The disagreement seen during the initial rise in temperature can be explained based on the nonhomogeneity of the batch. The model assumes the batch to be homogeneous at all times even in the presence of the solid phase, which is not completely justified. Besides, in the beginning the walls of the reactor contain a film of the viscous reaction mixture from the previous batch that also contains a large percentage of water. It is likely that such a film also exists on the thermocouple used to measure the batch temperature.

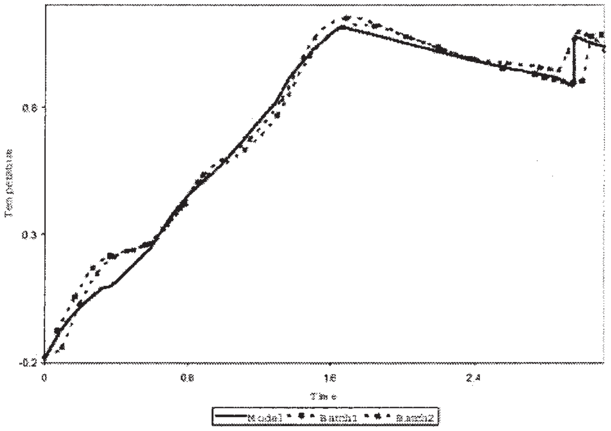

Figure 5. Temperature profile from the model is shown as a solid line, whereas the broken lines show the profiles obtained from two commercial batches.

The temperature and time have been filtered through a nonlinear technique to preserve the proprietary absolute values.

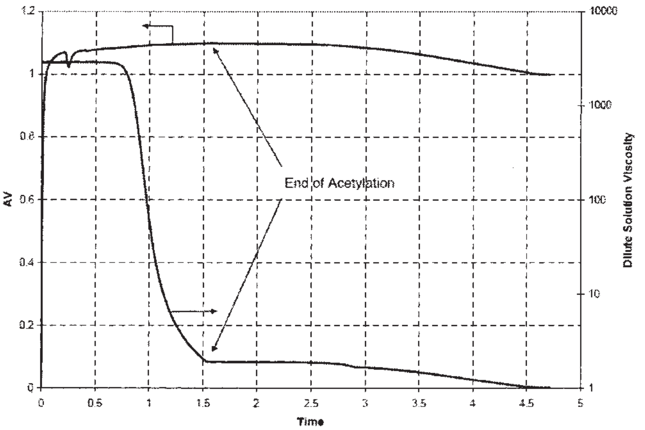

Figure 6. Overall acetyl value (AV) and dilute solution viscosity for acetylation followed by hydrolysis is plotted against time.

The x-axis is normalized by the peak time, whereas the y-axes are normalized by the observed average final values of AV and dilute solution viscosity.

The hydrolysis of acetic anhydride on the thermocouple itself can lead to its recording a misleading high temperature because the heat evolved from this reaction is not uniformly transferred to the batch. The mismatch in the profile after the peak temperature arises from the difference in time for the addition of the neutralizer. The second temperature rise is predicted correctly; however, the comparatively slow increase observed in the batches again most likely arises from other factors such as homogeneity.

Combined Process. To verify the accuracy of the combined model for acetylation and hydrolysis, we can compare the final properties of cellulose acetate as obtained by the model with the nominal values seen commercially. The two important properties that can be predicted by the model are the DP and the DA of cellulose. The degree of polymerization or DP of cellulose cannot be measured directly and is measured in the form of a dilute solution viscosity. Similarly, the degree of acetylation is measured by the acetyl value (AV) of cellulose that is defined as the weight fraction of the acetyl groups in cellulose units. From the stoichiometry, an equation for AV can be derived as

$$AV = \frac{6005 \times DA}{162.14 + 42 \times DA} \tag{23}$$

where *DA* is the degree of acetylation or the average number of hydroxyl groups substituted by the acetyl group per unit of cellulose.

The dilute solution viscosity and the AV of cellulose are plotted against the process time normalized by the peak time during acetylation (Figure 6). The *y*-axes have been normalized with the nominal values of the dilute solution viscosity and AV as observed in the final product of a commercial acetylation process with the same input streams as considered in the model. As can be seen the final values observed in the model are close to the observed values (corresponding to the *y*-axes values equal to 1). The end of the acetylation process is marked. The sensitivity of the acetylation process is evident from this figure, given that a large fraction of the changes take place during acetylation. The acetyl value in this plot reflects the acetyl substitution only in the liquid phase of the reaction. This explains the sudden increase initially in the AV of cellulose because for the model only a small fraction of cellulose is actually in the liquid phase when acetylation starts. Subsequently, the AV seems to level off before hydrolysis, despite acetyl substitution, because the amount of cellulose in the liquid phase increases as the solid cellulose dissolves. The hydrolysis of cellulose acetate can be seen as a less dynamic process that steers the cellulose properties to the required specifications.

Hydrolysis-based control

The training data for SVR was generated from the model of the process. The process with disturbances in the input streams of acetylation alone was simulated using the combined model to obtain a distribution of observable parameters of acetylation, peak temperature and peak time, and the resulting output variables, degree of acetylation and degree of polymerization. The input moisture content of the pulp was varied by changing the temperature and relative humidity of air during conveying as a 24-h cycle. The input temperature of the partially frozen mixture of sulfuric acid, acetic anhydride, and acetic acid was changed randomly and the mass of pulp charged in the reactor was assumed to vary as a Markov process: 500 data points were generated for training and 200 points for validation. A weak correlation exists between the peak temperature and the peak time and the output variables, DA and DP. The data were normalized between the maximum and the minimum values. A Multi Layer Perceptron (MLP) neural network with one hidden layer containing seven nodes was also trained on the same data. The choice of the number of layers and the nodes was based on the lack of significant improvement in the performance of the network when they were increased. The activation function used for the hidden layer was the tan-sigmoid transfer function. The network was trained using the Levenberg–Marquardt backpropagation (LMBP) algorithm. The function *newff* in the Matlab Neural Network Toolbox was used to create and train the network. Because of the requirement of a highly accurate prediction of DA and DP, the value of ε for SVM regression in Eq. 20 was fixed to 0 to make it more sensitive. The *quadprog* subroutine of Matlab was used for the optimization. The performance of SVM was found to be tolerant to small changes in the value of C in Eq. 20 and through trial and error that the value was fixed to be 500. A second-order polynomial function $K(\mathbf{x}_1, \mathbf{x}_2) = (1 + \mathbf{x}_1 \cdot \mathbf{x}_2)^2$ was found to perform the best as a kernel for predicting the DP, whereas the radial basis function (RBF) kernel $K(\mathbf{x}_1, \mathbf{x}_2) = \exp(-\|\mathbf{x}_1 - \mathbf{x}_2\|^2/\sigma^2)$ performed better for predicting the final DA of the batch. The value of the width (σ) of the RBF kernel was fixed as $\sqrt{10}$ through trial and error and the performance was found to be tolerant to small variations in this value. The process model, originally in FORTRAN, was converted into a Matlab DLL using the *mex* tool.

The mean of square errors of prediction divided by the variance of the degree of acetylation and polymerization of the validation data set for both the MLP neural network and SVR are presented in Table 2. The results obtained when linear regression is used on the same training and validation data sets are also presented for comparison. Note that the error of

Table 2. Mean of Square Errors of Prediction Divided by the Variance of Each Variable

Variable	MLP NN	SV Regression	Linear Regression
DA	0.83	0.99	1.25
DP	0.20	0.07	0.31

prediction for each validation point is not normalized. SVR outperforms Neural Networks in predicting DP and gives comparable results for DA. It is also observed and the DA of the output is more tolerant to disturbances during acetylation than DP. From the control perspective, it is thus more important to accurately predict DP for this problem. Based on these observations, SVR was chosen as the preferred prediction algorithm in the hydrolysis control strategy.

The process model was used to verify the effectiveness of the hydrolysis control strategy in controlling the output variables, DA and DP, of cellulose acetate. Disturbances in the input streams during acetylation, similar to those used to generate the training data for regression, were simulated. To start with, the parameters of the input stream, required for the hydrolysis model, were assumed to be known and the linear feedback assumption was not used. Equation 21 was used to evaluate the optimum quantities of the input streams of hydrolysis. Figure 7a shows the plot of DA and DP for 100 simulated batches. The results obtained by using hydrolysis control as well as baseline control (without using hydrolysis control) for each batch are shown for comparison. The axes are normalized by the nominal values of DA and DP. The region bound by the rectangle in the middle indicates the acceptable range for these parameters. In this particular set, 78 and 26% of the batches with and without control, respectively, lie inside the rectangle. From the simulations, it can be observed that the parameter DP is more sensitive than DA, which is more stable. The hydrolysis-based control algorithm balances the variability in these two parameters by increasing the spread in DA and reducing it for DP. It can be concluded from this plot that using the input streams of hydrolysis for control is an effective strategy to control the DA and DP of cellulose acetate. Note that these points represent simulated disturbances occurring simultaneously, which is a worst-case scenario. In reality, however, disturbances are less frequent and less severe in nature. Figure 8 shows how the optimum amounts of one of the neutralizer solutions and of water, which are added during hydrolysis, vary for the simulated batches. The *y*-axis is normalized by the nominal amounts of these streams in the process.

As mentioned earlier, given that the properties of the batch, before hydrolysis are not measured, a linear feedback assumption is made to use the prediction of the final DA and DP in hydrolysis control (Figure 4). To evaluate the validity of this assumption alone, batches were simulated with the assumption that only the final DA and DP are known exactly. Figure 7b shows the results obtained. In this set, 48 and 29% of the batches with and without control, respectively, lie inside the rectangle. Although the results of hydrolysis control have comparatively reduced in efficacy as a result of the linear feedback assumption, points are still closer to the acceptable range than those of batches without control, which shows that this assumption can be feasibly used to control the DA and DP of the product.

To further extend the approach, we performed the simulations using the trained SVR to predict the final DA and DP from the peak temperature, peak time, and the second temperature rise, observed during acetylation. The optimum values of the input streams to be added during hydrolysis were obtained from Eq. 22. These input streams are applied to the batch during hydrolysis. Figure 9a shows the DA and DP plotted for 100 batches with randomly simulated disturbances. The results of the same batches, without hydrolysis control, are also shown for comparison. In this particular set, 43% of the points with hydrolysis control are within the acceptable range compared to 33% for the case of no control. On comparing these results with those of Figure 7b, it can be concluded that the inaccuracy in our prediction is sufficiently low such that it does not affect our results.

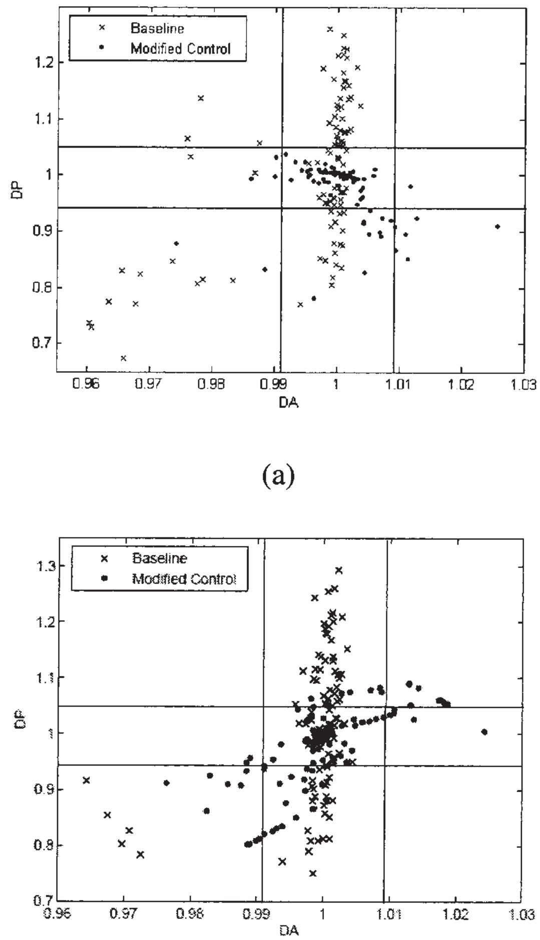

(a)

(b)

Figure 7. Degree of acetylation (DA) and degree of polymerization (DP) for 100 simulated batches with disturbances during acetylation for baseline conditions (×) and with modified control (●) when (a) the input batch parameters for hydrolysis are known and (b) when only the final values of DA and DP for the final batch are known.

Data were normalized with the target DA and DP values and the lines represent the acceptable range for these parameters.

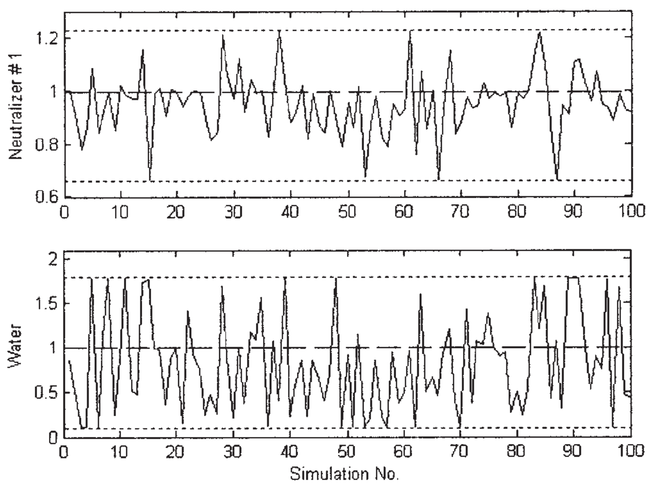

Figure 8. Amount of two different input streams during hydrolysis, as evaluated by the hydrolysis control, for 100 simulation runs.

The y-axes are normalized with nominal amounts of these two streams and the upper and lower bounds are indicated by the dotted lines.

To further improve this approach, we can modify the penalty function to be minimized in Eq. 22. Because the batch parameters within a given range, as seen in Figure 9a, are acceptable, the objective function should aim to converge the points within that range instead of a specific target value. This is achieved by using the following objective function:

$$\min \beta\{DA_{target} - [DA^{p}(a) - DA_{target}^{ub \text{ or } lb}] - DA^{n}(x)\}^2 + \{DP_{target} - [DP^{p}(a) - DP_{target}^{ub \text{ or } lb}] - DP^{n}(x)\}^2 \quad \text{subject to } lb \le x \le ub \tag{24}$$

where $DA_{target}^{ub \text{ or } lb}$ and $DP_{target}^{ub \text{ or } lb}$ imply the corresponding upper or lower bounds of DA and DP depending on the one that is violated by the predicted value. If the prediction lies within the bounds, the difference is set to 0. Note that the other target term in the expression remains the same. Figure 9b shows the results obtained from the modified objective function. In this set, 64% of the points with hydrolysis control conform to the acceptable range compared to 39% of the points without any control. The application of hydrolysis-based control clearly improves the quality of the batches.

In actual cellulose acetate synthesis, batches from different reactors working in parallel are usually blended and the properties measured are an average of the individual reactors. Such a procedure can improve the apparent properties of the batch because the disturbances occurring in individual units can cancel when averaged. To observe the effect of implementing the hydrolysis-based control on the blended batch, a batch consisting of nine parallel units was simulated. The disturbances in each of the units were assumed to be independent of each other. Figure 10 shows a set of results from 100 batches, each being a blend of nine units. The acceptable range, which was broad in the simulations of the single units, is narrower for a blended product. A bias can be observed when hydrolysis control is applied to the batches, which is expected following Figure 9b. This bias is in fact ascribed to the underlying linear assumption of the hydrolysis model while designing this strategy. Some 56% of the data without control are located inside the acceptable range after blending compared to 59% of the data with hydrolysis control. Although the properties of the batch without control show a large improvement, note that blending does not improve the batch properties such as degree of polymerization at the molecular level, which may be significant for further downstream processes. Hydrolysis control, on the other hand, can improve the properties of each individual batch.

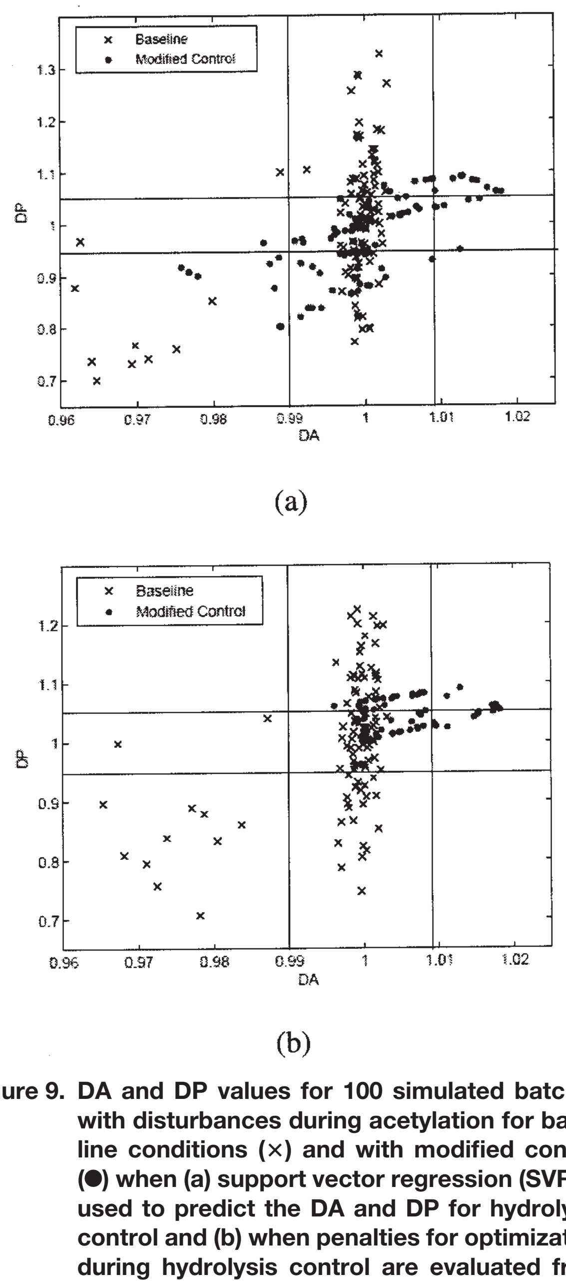

Figure 9. DA and DP values for 100 simulated batches with disturbances during acetylation for baseline conditions (×) and with modified control (●) when (a) support vector regression (SVR) is used to predict the DA and DP for hydrolysis control and (b) when penalties for optimization during hydrolysis control are evaluated from the edges of the box.

Data were normalized with the target DA and DP values and the lines represent the acceptable range for these parameters.

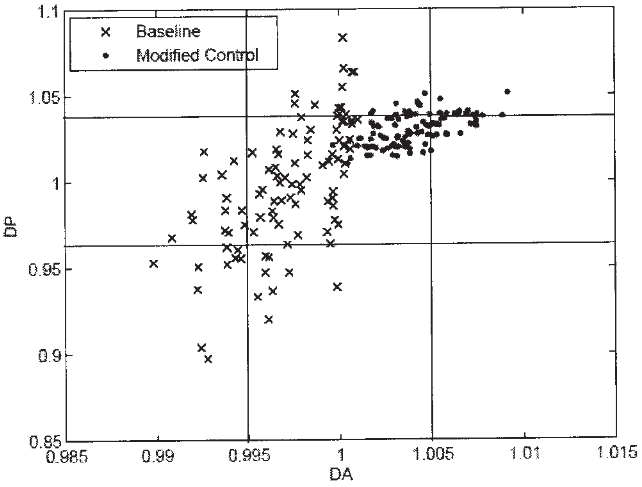

Figure 10. Degree of acetylation (DA) and degree of polymerization (DP) for 100 batches, each batch constituting a blend of nine separate batches with simulated disturbances during acetylation for baseline conditions (×) and with modified control (●).

Data were normalized with the target DA and DP values for the batch and the lines represent the acceptable range for these parameters.

Conclusions

The acetylation of cellulose is divided in two steps: acetylation and hydrolysis. The temperature profile for these steps, as predicted by the model, matches well with the observed commercial profile, particularly the peak time and the peak temperature. The novel features of the acetylation model include the dissolution of the cellulose fiber through sulfation, the melting of the ice, and the elaborate heat transfer. The assumptions of the sulfation reaction as a mass transfer limited process and of the fractional units of cellulose that dissolve with the sulfation are justified by the accurate prediction of the peak time that depends critically on the rate of dissolution of cellulose. Similarly, the correct prediction of peak temperature justifies the heat balance of the system, which mainly includes the thermal changes in the batch. The heat taken up by the vessel and the contribution of the stirrer are also found to be significant for the heat balance. When the acetylation model is combined with an improved hydrolysis model, the final product properties predicted agree well with those observed in the plant. This further validates the acetylation model and also provides the means to predict the effect that changes during acetylation has on the final product specifications.

Several disturbances can occur during acetylation that affect the final properties of cellulose acetate, making it more variable for subsequent processing. Based on the model of the process, an inferential intrabatch control strategy was developed, which uses the input streams during hydrolysis to counter various disturbances that occurred during acetylation. No disturbances were assumed to occur during the hydrolysis process. Results showed that this strategy can successfully control the final degree of acetylation (DA) and degree of polymerization (DP) of cellulose acetate within the expected ranges.

Because the constitution and properties of the stream that enters for hydrolysis after acetylation are not measured in the plant, a linear feedback assumption was used for the hydrolysis model.

Support vector regression (SVR) was used to predict the final DA and the DP of cellulose acetate from the observed parameters during acetylation. This prediction was used to evaluate the control action. The model was used to generate the data assuming random disturbances during the acetylation process, which was used to train the SVR. The results, from simulating the modified control strategy, show improved final DA and DP of the batches under random disturbances. Thus, it can be concluded that this strategy effectively controls two of the main batch properties.

Acknowledgments

The authors gratefully acknowledge Celanese Acetate, LLC for providing the funding and the necessary data for this research.

Notation

b, b^* = bias of SVM, optimized value
$c_{p,i}$ = molar specific heat capacity of species i
$C_{AAc}^{Eq}(T)$ = equilibrium interface concentration of acetic acid at T
D = diffusion coefficient of AAc into the solution from the ice crystals
D_{eff} = effective diffusion coefficient for water into cellulose particles
$DA(x)$, $DP(x)$ = DA, DP with x amounts of streams in hydrolysis
$DA^{n}(x)$ = $DA(x)$ with no disturbances in acetylizer
$DA^{p}(a)$ = DA as predicted by SVR with nominal amounts of streams, a, during hydrolysis
$F_{i,j}$ = molar flow rate of ith species in jth stream
$\Delta H_{r,k(T)}$ = enthalpy of kth reaction at temperature T
$K(\mathbf{x}, \mathbf{z})$ = kernel function for vectors **x** and **z**
m = order of the polynomial kernel
m_i = moles of the ith species in the reactor
$\dot{Q}$ = external sources of heat to the reactor
R_k = molar rate of reaction k
T_j = temperature of stream j
$v_{i,k}$ = stoichiometric coefficient of species i in reaction k
w_{AAc}^{Eq} = equilibrium interface weight fraction of AAc at T

Greek letters

α, α^* = Lagrangian variable, optimized value
β = scaling factor of AV in hydrolysis control
ε = loss sensitivity for SVR
$\phi(\mathbf{x})$ = transformed feature vector for **x**
ξ = moles of steam required per unit increase of batch temperature
σ = width of the RBF kernel

Acronyms

AAc = acetic acid
AV = acetyl value of cellulose
DA = degree of acetylation of cellulose
DP = degree of polymerization of cellulose
RBF = radial basis function
SVM = support vector machine
SVR = support vector regression

Literature Cited

1. Joseph B, Brosilow CB. Inferential control of processes. *AIChE J.* 1978;24:485-508.
2. Morari M, Fung AKW. Nonlinear inferential control. *Comput Chem Eng.* 1982;6:271-281.
3. Doyle I, Francis J. Nonlinear inferential control for process applications. *J Process Control.* 1998;8:339-353.

4. Azlan Hussain M. Review of the applications of neural networks in chemical process control—Simulation and online implementation. *Artif Intell Eng.* 1999;13:55-68.
5. Christianini N, Shawe-Taylor J. *An Introduction to Support Vector Machines and Other Kernel-Based Learning Methods*. Cambridge, UK: Cambridge Univ. Press; 2000.
6. Vapnik V. *The Nature of Statistical Learning Theory*. Berlin, Germany: Springer-Verlag; 1995.
7. Deniz O, Castrillon M, Hernandez M. Face recognition using independent component analysis and support vector machines*1. *Pattern Recogn Lett.* 2003;24:2153-2157.
8. Sanchez VD. Advanced support vector machines and kernel methods. *Neurocomputing.* 2003;55:5-20.
9. Suykens JAK, Vandewalle J, De Moor B. Optimal control by least squares support vector machines. *Neural Networks.* 2001;14:23-35.
10. Yan W, Shao H, Wang X. Soft sensing modeling based on support vector machine and Bayesian model selection. *Comput Chem Eng.* 2004;28:1489-1498.
11. Malm CJ, Tanghe LJ. Chemical reactions in the making of cellulose acetate. *J Ind Eng Chem.* 1955;47:995-999.
12. Araki T. Cellulose acetate. III. Combination of sulfuric acid during the acetylation of cellulose and the mechanism of acetylation. *Textile Res J*. 1952;22:630-636.
13. Malm CJ, Tanghe LJ, Laird BC. Preparation of cellulose acetate-action of sulfuric acid. *J Ind Eng Chem*. 1946;38:77-82.
14. Tang L-G, Hon DNS, Zhu Y-Q. An investigation in solution acetylation of cellulose by microscopic techniques. *J Appl Polym Sci*. 1997; 64:1953-1960.
15. Malm CJ, Tanghe LJ, Schmitt JT. Catalysts for acetylation of cellulose. *J Ind Eng Chem.* 1961;53:363-367.
16. Malm CJ, Tanghe LJ, Laird BC, Smith GD. Relative rates of acetylation of the hydroxyl groups in cellulose acetate. *J Am Chem Soc.* 1953;75:80-84.

Manuscript received Aug. 15, 2005, and revision received Feb. 5, 2006.